ASTRONOMY & ASTROPHYSICS
SUPPLEMENT SERIES

JULY **1994**, PAGE 29

Astron. Astrophys. Suppl. Ser. **106**, 29-37 (1994)

Three-year monitoring of a sample of flat-spectrum radio sources at 327 MHz*

T. Ghosh[1,2,**], Gopal-Krishna[3] and A.P. Rao[3]

[1] Radio Astronomy Centre, P.O. Box 8, Udhagamandalam 643 001, India
[2] Joint Astronomy Programme, Department of Physics, Indian Institute of Science, Bangalore 560 012, India
[3] National Centre for Radio Astrophysics, T.I.F.R. P.O. Bag 3, Pune University Campus, Ganeshkhind, Pune 411 007, India

Received November 17, 1993; accepted February 8, 1994

Abstract. — Results of a 3-year monitoring programme at 327 MHz with the Ooty Synthesis Radio Telescope are presented. The majority of the sample consists of BL Lac objects, high-optical polarization quasars (HPQ) and low-optical polarization quasars (LPQ). In addition, a few known variable sources, GHz-peaked spectrum sources and compact doubles were also added. Including an additional set of 36 control and calibrator sources, a total of 82 sources were observed at roughly 3-month intervals for about 3 years. We find 19 variable and 6 possibly-variable sources. However, the observed variability in the BL Lac-HPQ-LPQ subsamples does not seem to be influenced by their optical properties.

Key words: active galactic nuclei — radio sources — low frequency variability

1. Introduction

Compact extragalactic radio sources are known to undergo strong intensity variations below 1 GHz over time scales of months to years (low-frequency variability – LFV). Two major scenarios explaining this phenomenon are (e.g. Padrielli et al. 1987):

- refractive interstellar scintillation (RISS) caused by large-scale irregularities in the interstellar medium (ISM). It has been argued that the intergalactic medium could also contribute significantly to the observed LFV of blazars (Gopal-Krishna 1991).
- Doppler boosting due to bulk relativistic motion of radio-emitting plasmons along a direction close to the line-of-sight.

In an attempt to find observational evidence supporting either of these two views, we monitored the 327-MHz flux densities of a sample of flat-spectrum radio sources over a period of three years. The sample contained examples with different optical properties, most sources being classified as BL Lac objects, or optically high- or low-polarization quasars. The prime objective was to find whether the observed variability is different among these three different classes and how the results compare with variations at other frequencies. In a previous paper (Ghosh & Gopal-Krishna 1990, Paper I) we have discussed our interpretation of the results, while here we present the details of the flux-density monitoring.

2. The sample

Between 1985 and 1988, we monitored the 327-MHz flux densities of a carefully-chosen sample of flat-spectrum extragalactic radio sources using the Ooty Synthesis Radio Telescope (OSRT, Swarup 1984; Sukumar et al. 1988). The sample consists of 8 BL Lac objects from Weiler & Johnston (1980), 17 high-optical-polarization quasars (HPQ, with polarization greater than 3%) from Moore & Stockman (1981, 1984) and 9 low optical-polarization quasars (LPQ) from Stockman et al. (1984). All sources satisfy the following criteria:

i) flat radio spectrum at decimetre wavelength ($\alpha \geq -0.5$; where $S_\nu \propto \nu^\alpha$).
ii) $|\delta| \leq 35°$, so that the sources lie within the pointing range of the OSRT.
iii) $|b^{\rm II}| \geq 10°$, selecting lines-of-sight well away from the galactic plane, and thus minimizing the predicted variations of scattering effects with galactic longitude.

* Tables 1 to 2 are also available in electronic form: see the Editorial in A&AS, 1994, Vol. 103, No.1

** *Present address*: Arecibo Observatory, P.O. Box 995, Arecibo, Puerto Rico 00613

iv) $S_{327} \geq 1$ Jy as estimated from interpolation/extrapolation of the spectrum. This criterion implies that the selected sources are strong enough to be measured with good signal-to-noise ratios.

v) evidence of a dominant compact core at 327 MHz, based on published interplanetary-scintillation or *VLBI* observations at metre wavelengths. It is well established that sources lacking compact components do not vary (Condon et al. 1979).

vi) no confusing sources with $S_{327} > 0.7$ Jy within the effective OSRT field of view of 7×170 arcmin^2, for reasons described in Sect. 3.

A few additional objects of special interest were added to this compact-source sample during the course of monitoring. Of these, seven are known variable sources (Fanti et al. 1981), one is a GHz-peaked-spectrum (GPS) source (Carvalho 1985), three are compact doubles (CDs from Phillips & Mutel 1982 and Hodges et al. 1984) and one source, 1748-253, that is seen through the near-galactic centre region ($l = 4°.0$, $b = 0°.6$). The main sample consisting of BL Lac objects, HPQs and LPQs was used for the statistical analysis of Paper I, source selection being unbiased towards any previous history of variability.

A group of 25 strong ($S_{327} > 6$ Jy), steep-spectrum sources with no known history of low frequency variability was also selected from the OSRT calibrator list. These sources were used both as flux-density calibrators and as a control sample. However, the median flux density of this calibration/control sample was much stronger than the sources in the compact sample. Hence, to check the internal consistency of our observing and analysis procedure, another sample of 11 steep-spectrum double sources were added to the monitoring programme in 1987. The median flux density of this set was 1.7 Jy, which is very similar to the median flux density of the compact-source sample. These had angular sizes in the range 7 to 12 arcsec (Lawrence et al. 1986), and were hence unresolved by the OSRT. Double sources in this angular-size range are not expected to show intensity fluctuations due to RISS.

3. Observations and data reduction

Both the compact-source sample and the calibrator/control sample were observed at roughly three-months interval between April 1985 and January 1988 using the OSRT. A detailed description of the telescope is given by Sukumar et al. (1988) and the observing and reduction method has been discussed in detail in Ghosh & Rao (1992). Here, we shall present only a brief description.

The OSRT is an Earth-rotation synthesis telescope consisting of five separate sections of the parabolic cylinder of the Ooty Radio Telescope (ORT, Swarup et al. 1971), each sector measuring 30×100 m^2, and seven smaller cylinders of size 9×23 m^2 distributed over a 4-km diameter area.

With the large number of sources in our sample, full synthesis mapping was not possible since a duration of only about 2 hr could be allowed per source in each observing session. At each epoch, the observations were spread over 4-5 days. Since the sources were distributed over all right ascensions, the observations were taken continuously over the entire observing session. Both compact sources and control sources were treated identically. Three or four 30-min scans, well separated in hour angle, were recorded for each source. The schedule was set up such that at least one 5-min calibrator scan was taken every hour. However, mapping and estimating flux densities from these snap-shot data proved unreliable as:

- self-calibration techniques could not be applied for sources of about 1-Jy strength owing to both low signal-to-noise ratio for all pairs of small antennae, and the poor UV coverage,
- the ORT-sections and the small antennae have very different fields of view causing different levels of confusion and leading to large baseline-dependent errors.

Instead, we have estimated flux densities using only the measured visibility amplitudes. The method is based on the principle of broken-coherence averaging (Thompson et al. 1986), which is frequently used in *VLBI* data analysis. The calibration of the visibility amplitudes was achieved from the ensemble of the calibrator observations in a session. The visibility data for the calibrators were used to derive the antenna-based amplitude gains. The moduli of these estimated gains were then plotted against declination for all calibrators and fitted with the theoretical declination dependence of the antenna gains. These fitted curves for each antenna were then used to convert the correlation coefficients into flux densities in Jy. Using this procedure, the amplitude calibration was no longer critically dependent on the assumed flux density for any particular calibrator which can differ from the actual value due to either variability or measurement error.

Using the 5-min calibrator scans recorded once per hour, the antenna-based phases were also determined. As the coherence time of intra-ORT baselines was more than 1 hour, phase calibration once per hour was quite adequate for the ORT sections. After applying the calibration for the five ORT sections, the phases on all five baselines involving the 5 ORT sections and a single small antenna tracked one another closely. These were then added coherently, giving the visibility which would have been seen by an interferometer consisting of the full ORT and the particular small antenna. This procedure reduced the field of view to 7×170 arcmin^2 from its usual value of 40×170 arcmin^2. This also reduced both thermal and confusion noise on the averaged visibility derived for each of these modified baselines. The resultant signal-to-noise ratio for a 5-min measurement on each baseline was now better than 5:1 for a 1 Jy source, enabling us to ignore the noise-bias effect and regard the observed visibility amplitudes as having a Gaussian distribution about the true value of the source flux density. The fact that there were no strong confusing sources within the effective field-of-view strengthened this assumption (see selection criterion vi). The total error on such a measurement (for a particular scan) is made up of thermal and confusion noise (ϵ_1), plus a calibration error (ϵ_2) proportional to the flux density of the target source originating from the uncertainties in the gain-declination fits. Using all the 5-min scans on the control and calibration sources over the entire period of monitoring, we have found that the value of ϵ_1 is about 100 mJy, while ϵ_2 is declination-dependent, being about 5% for sources with $|\delta| \leq 15°$ and 7% for $|\delta| > 15°$. Since all sources were unresolved by the OSRT, no reduction in visibility amplitude with increasing baseline was expected. The flux-density estimates for a particular epoch presented here are the average of these visibility amplitudes estimated during a given observing session. The associated error is further reduced by a factor of $\sqrt{N}$, where N is the number of scans on all averaged baselines. To investigate any epoch-dependence of the gain calibrations we have calculated the percentage deviation from the mean flux density (over the three-year period) of each calibration source at each observing epoch. The mean percentage deviation at each epoch was $\leq$ 3.8%, with none differing from zero with a significance $> 2.3\sigma$.

4. Results

In Tables 1 and 2, we present the 327-MHz flux densities at each epoch for the compact-source and the control/calibrator samples, respectively.

The variance of the measured flux densities of a source is the squared sum of terms representing the true source variations, σ_s and the measurement errors, ϵ:

$$\sigma_o^2 = \sigma_s^2 + \epsilon^2 \tag{1}$$

Therefore, we parametrize the degree of flux-density variations by the corrected variability index, defined as:

$$m_c = \left[\left(\sigma_o^2 - \epsilon^2\right)^{1/2} / \mu_s\right] \times 100\% \tag{2}$$

where, σ_o^2 is the weighted variance of the measured flux densities of a source, S_i, and is defined as:

$$\sigma_o^2 = \frac{N \sum \left[\omega_i' \left(S_i - \mu_s\right)^2\right]}{(N-1) \sum \omega_i'} \tag{3}$$

and, μ_s is the weighted-mean flux density defined as:

$$\mu_s = \frac{\sum (\omega_i' S_i)}{\sum \omega_i'} \tag{4}$$

The weights are determined from the individual measurement errors (σ_i') as:

$$\omega_i' = \frac{1}{\sigma_i'^2} \tag{5}$$

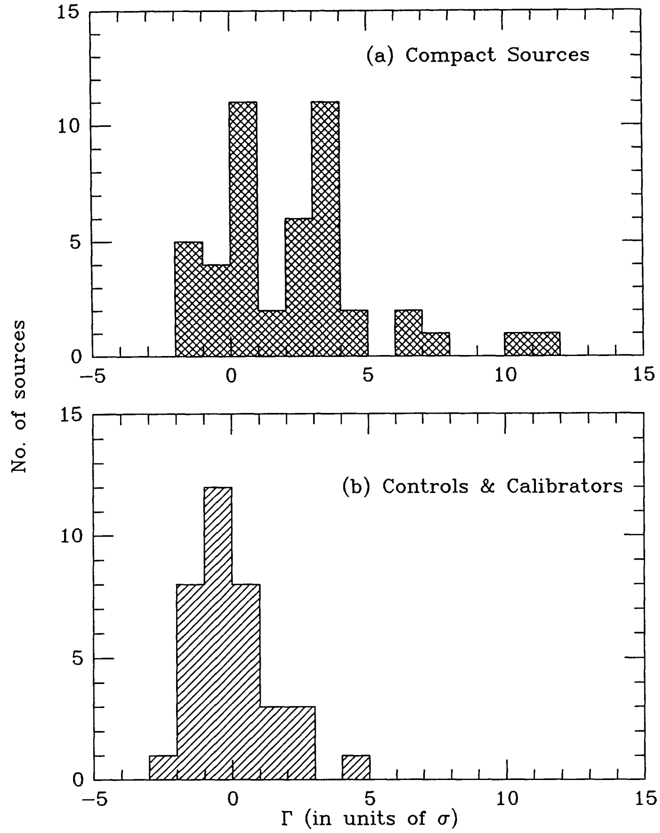

Fig. 1. Histograms of the statistical significance of the measured variations (Γ) for; a) the compact-source sample and b) the control and calibrator sample

The error term in Eq. (1) is obtained from: $\epsilon^2 = 100^2 + (\epsilon_2 \times \mu_s)^2$, in mJy, where ϵ_2 is 0.05 for sources with $|\delta| \leq 15°$ and 0.07 for sources with $|\delta| > 15°$.

In the absence of any true source variability, σ_o will have a Gaussian distribution about ϵ, with a standard deviation of $\epsilon/\sqrt{(2N)}$. Hence, to find the statistical significance of the measured variations, we calculate the following quantity:

$$\Gamma = \frac{\sigma_o - \epsilon}{\epsilon/\sqrt{(2N)}} \tag{6}$$

We consider a source to be variable (V), only if $\Gamma \geq 3$, and possibly variable (PV) when $2 \leq \Gamma < 3$. All other sources are considered to be non-variable (NV), as found during the period of our monitoring, and we quote an upper limit for their variability indices by calculating:

$$v^2 = \left(\epsilon + 3\epsilon/\sqrt{(2N)}\right)^2 - \epsilon^2 \quad (7)$$

$$v = \sqrt{\left(6\sqrt{(2N)} + 9\right)} \times \frac{\epsilon}{\sqrt{(2N)}} \quad (8)$$

in percentage of the mean flux density (μ_s) of the source.

In Fig. 1, we plot the histograms of Γ for both the compact-source sample and the control/calibrator sample. The control/calibrator sample shows a symmetric distribution about $\Gamma = 0$ within 3σ, while the positive tail for the compact sources, seen extending up to 12 σ, clearly demonstrates the existence of true source variability in this sample. As discussed in detail in Paper I, we find that the three optical types (i.e. BL Lacs, HPQs and LPQs) have very similar median values for m_c of about 12%. This would seem to imply that the measured low-frequency variability is consistent with the propagation scenario in which any source having milli-arcsec angular size is expected to undergo low-frequency intensity fluctuations due to refractive scattering, regardless of its other intrinsic properties (see Paper I).

Acknowledgements. We thank the staff of the Radio Astronomy Centre for their help during the observations and Chris Salter for a critical reading of the manuscript.

References

Carvalho J.C. 1985, MNRAS 215, 463
Condon J.J., Ledden J.C., O'Dell S.L., Dennison B. 1979, AJ 84, 1
Fanti C., Fanti R., Ficarra A., Mantovani F., Padrielli L., Weiler K.W. 1981, A&AS 45, 61
Ghosh T., Gopal-Krishna 1990, A&A 230, 297
Ghosh T., Rao A.P. 1992, A&A 264, 203
Gopal-Krishna 1991, Current Sci. 60, 117
Hodges M.W., Mutel R.L., Phillips R.B. 1984, AJ 89, 1327
Lawrence C.R., Bennett C.L., Hewitt J.N., Langston G.I., Kloty S.E., Burke B.F. 1986, ApJS 61, 105
Moore R.L., Stockman H.S. 1981, ApJ 243, 60
Moore R.L., Stockman H.S. 1984, ApJ 279, 465
Padrielli L., Aller M.F., Aller H.D. et al. 1987, A&AS 67, 63
Phillips R.B., Mutel R.L. 1982, A&A 106, 21
Stockman H.S., Moore R.L., Angel J.R. 1984, ApJ 279, 485
Sukumar S., Velusamy T., Rao A.P. et al. 1988, Bull. Astron. Soc. India 16, 93
Swarup G., Sarma N.V.G., Joshi M.N. et al. 1971, Nat. Phys. Sci. 230, 185
Swarup G. 1984, JA&A 5, 139
Thompson A.R., Moran J.M., Swenson G.W. 1986, Interferometry and Synthesis in Radio Astronomy (John Wiley and Sons, New York)
Weiler K.W., Johnston K.J. 1980, MNRAS 190, 269

Table 1. Flux-density measurements for the compact-source sample

Source	Type	Epoch	S_{327} (mJy)	Error (mJy)	Epoch	S_{327} (mJy)	Error (mJy)	m_c%	Γ	Comment
0048−097	BL	08Feb86	781.2	107.4	16Dec86	834.4	108.4	< 20.5	-1.8	NV
		16May86	838.1	108.4	08Jan88	864.0	108.9			
		24Aug86	923.8	110.2						
0122−003	LPQ	08Feb86	815.0	108.0	16Dec86	1028.3	112.4	< 17.3	0.9	NV
		16May86	1098.1	114.1	28Sep87	1173.2	115.9			
		24Aug86	1122.9	114.7	10Jan88	895.8	109.6			
0202+149		08Feb86	6247.9	328.0	16Dec86	4472.2	245.0	15.4	3.8	V
		24Aug86	5918.4	312.4	09Jan88	4609.0	251.2			
0235+164	BL	28Sep85	908.0	118.5	18Dec86	883.9	117.6	20.4	2.9	PV
		24Aug86	1180.3	129.7	08Jan88	1443.3	142.2			
0237−233	GPS	28Sep85	2347.1	192.3	18Dec86	2786.0	219.2	< 11.7	0.6	NV
		08Feb86	3021.1	233.9	03Apr87	2977.5	231.2			
		16May86	2747.5	216.8	08Jan88	3017.3	233.7			
		24Aug86	2632.0	209.6						
0336−019	HPQ	14May85	1293.3	119.1	30Mar87	1755.5	133.1	15.8	3.7	V
		08Feb86	1343.1	120.5	28Sep87	1431.7	123.0			
		24Aug86	981.1	111.4	09Jan88	1143.6	115.2			
		18Dec86	1229.7	117.4						
0420−014	HPQ	10May85	929.2	110.3	26Mar87	970.9	111.2	< 17.4	-0.3	NV
		08Feb86	918.0	110.0	28Sep87	1135.5	115.0			
		24Aug86	797.1	107.7	11Jan88	1016.1	112.2			
		17Dec86	942.8	110.6						
0422+005		12May85	737.7	106.6	17Dec86	820.3	108.1	< 21.1	-1.8	NV
		08Feb86	870.8	109.1	24Mar87	746.4	106.7			
		24Aug86	810.8	107.9	11Jan88	840.7	108.5			
0430+052		08Feb86	4306.2	237.4	17Dec86	3812.7	215.3	< 10.1	0.3	NV
3C120		23Aug86	3863.3	217.5	24Mar87	3739.7	212.0			
0458−020	HPQ	14May85	2133.3	146.2	23Aug86	2368.9	155.0	< 9.5	0.8	NV
		27Sep85	2095.6	144.8	17Dec86	2639.3	165.6			
		08Feb86	2399.7	156.2	24Mar87	2525.8	161.1			
		16May86	2272.7	151.4	29Sep87	2365.5	154.9			
0605−085	HPQ	09Feb86	3542.8	203.4	24Mar87	2750.6	170.0	11.1	3.9	V
		16May86	2742.3	169.7	29Sep87	2457.3	158.4			
		22Aug86	2465.8	158.8	09Jan88	2630.5	165.2			
		19Dec86	3061.5	182.9						
0607−157		09Feb86	1426.0	122.8	24Mar87	743.1	106.7	26.0	4.6	V
		16May86	1063.9	113.3	29Sep87	833.6	108.3			
		22Aug86	556.7	103.8	09Jan88	924.0	110.2			
		19Dec86	968.6	111.1						
0735+178	BL	15May85	1740.3	157.6	17Dec86	1685.6	154.7	11.2	2.3	PV
		09Feb86	2117.0	178.8	02Oct87	2191.7	183.1			
		16May86	2310.8	190.2	10Jan88	1821.1	162.0			
		22Aug86	1606.0	150.5						
0736+017	HPQ	09Feb86	1677.0	130.5	22Aug86	1576.7	127.3	< 13.9	-0.7	NV
		16May86	1676.0	130.5	19Dec86	1813.4	135.0			
0738+313	LPQ	26Sep85	1794.7	160.6	22Aug86	1724.7	156.8	< 15.0	-0.1	NV
		09Feb86	1425.8	141.3	19Dec86	1546.1	147.4			
		16May86	1642.2	152.4						
0851+202	BL	15May85	773.5	113.7	28Mar87	1132.7	127.6	< 17.5	1.2	NV
OJ287		10Feb86	1124.9	127.3	29Sep87	1145.7	128.2			
		12May86	1260.0	133.3	08Jan88	980.6	121.3			
		20Dec86	1150.3	128.4						
0906+015	HPQ	29Apr85	775.8	107.3	20Dec86	903.0	109.7	< 18.2	1.8	V
		15May85	651.7	105.2	25Mar87	1110.9	114.4			
		10Feb86	793.8	107.6	05Oct87	607.8	104.5			
		12May86	899.4	109.7	08Jan88	786.7	107.5			

Table 1. continued

Source	Type	Epoch	S_{327} (mJy)	Error (mJy)	Epoch	S_{327} (mJy)	Error (mJy)	m_c%	Γ	Comment
1038+064	LPQ	29Apr85	1456.4	123.7	19Dec86	1502.3	125.1	11.4	2.3	PV
		09May85	1536.7	126.1	20Mar87	1064.4	113.3			
		09Feb86	1302.4	119.3	11Jan88	1158.9	115.6			
		12May86	1526.7	125.8						
1055+018	HPQ	09May85	4426.3	242.9	19Dec86	4593.9	250.5	< 8.6	-1.3	NV
		10Feb86	4422.0	242.7	20Mar87	4753.8	257.9			
		12May86	4465.8	244.7	11Jan88	4314.4	237.8			
1117+146		07Feb86	3138.1	186.1	20Mar87	2975.0	179.2	10.7	3.3	V
		16May86	2542.5	161.7	28Jan88	3528.3	202.8			
		18Dec86	2795.6	171.9						
1156+295	HPQ	25Apr85	3258.0	249.0	18Dec86	3637.9	273.6	30.2	11.2	V
		07Feb86	3988.9	296.6	27Mar87	3472.2	262.8			
		16May86	1725.8	156.8	08Jan88	3567.5	269.0			
		22Aug86	2958.3	230.0						
1219+285	BL	25Apr85	1322.1	136.3	18Dec86	1663.3	153.5	15.3	3.2	V
		07Feb86	1522.2	146.1	20Mar87	1448.3	142.4			
		16May86	1771.2	159.3	08Jan88	1003.3	122.2			
		22Aug86	1435.2	141.8						
1226+023	LPQ	26Apr85	63483.6	3175.8	18Dec86	58340.0	2918.7	< 7.5	0.2	NV
3C273		07Feb86	62893.3	3146.3	26Mar87	69250.0	3463.9			
		17May86	60459.6	3024.6	08Jan88	62572.2	3130.2			
		22Aug86	63716.8	3187.4						
1253−055	HPQ	25Apr85	11408.5	579.1	22Aug86	15063.9	759.8	12.9	6.0	V
3C279		07Feb86	14522.2	733.0	20Mar87	16556.7	833.9			
		17May86	15289.6	771.0	08Jan88	13011.1	658.2			
1502+106	HPQ	11May85	705.8	106.0	25Dec86	922.4	110.1	< 17.1	0.4	NV
		29Sep85	776.8	107.3	28Mar87	896.1	109.6			
		12Feb86	1078.8	113.6	29Sep87	989.0	111.6			
		15May86	762.2	107.0	10Jan88	886.7	109.4			
		23Aug86	965.8	111.1						
1504−166	HPQ	12Feb86	1087.5	125.7	28Mar87	1403.9	140.2	16.4	3.3	V
		15May86	1006.4	122.3	29Sep87	1360.0	138.1			
		23Aug86	1226.1	131.8	10Jan88	1731.9	157.2			
		25Dec86	1575.4	148.9						
1510−089	HPQ	11May85	2747.5	169.9	24Dec86	2360.8	154.7	9.9	3.5	V
		24Sep85	2629.2	165.2	24Mar87	2607.8	164.3			
		12Feb86	2510.1	160.5	29Sep87	2129.7	146.1			
		14May86	2083.1	144.4	10Jan88	2005.0	141.6			
		23Aug86	2636.3	165.5						
1514−241	BL	28Apr85	1571.2	148.7	24Dec86	1900.3	166.4	11.4	2.7	PV
		24Sep85	1918.0	167.4	20Mar87	1859.4	164.1			
		12Feb86	2473.0	200.0	29Sep87	1521.1	146.1			
		18May86	2025.7	173.5	10Jan88	1964.2	170.0			
		23Aug86	2064.1	175.7						
1518+047	CD	26Apr85	1833.1	135.7	23Aug86	1793.3	134.4	10.8	3.2	V
		24Sep85	2543.3	161.8	22Dec86	2061.0	143.6			
		12Feb86	1782.9	134.0	29Sep87	1902.0	138.0			
		18May86	1937.9	139.2	10Jan88	1650.0	129.6			
1524−136		12Feb86	5353.8	285.8	23Dec86	5526.0	293.8	< 8.3	0.1	NV
		18May86	6060.0	319.1	26Sep87	6023.8	317.4			
		23Aug86	5398.9	287.9	10Jan88	5822.8	307.8			
1538+149	BL	28Apr85	2184.6	148.1	24Dec86	2657.5	166.3	< 12.0	0.2	NV
		28Sep85	2818.9	172.8	27Mar87	2411.0	156.6			
		12Feb86	2628.7	165.2	29Sep87	2396.9	156.1			
		23Aug86	2558.8	162.4						
1546+027	HPQ	28Apr85	417.5	102.2	26Dec86	569.4	104.0	< 28.3	0.4	NV
		12Feb86	367.5	101.7	26Mar87	487.8	102.9			
		18May86	461.4	102.6	29Sep87	562.2	103.9			
		22Aug86	644.4	105.1	10Jan88	703.6	106.0			

Table 1. continued

Source	Type	Epoch	S_{327} (mJy)	Error (mJy)	Epoch	S_{327} (mJy)	Error (mJy)	m_c%	Γ	Comment
1607+268	CD	28Apr85	2050.2	174.9	23Aug86	2424.4	197.0	< 13.4	0.9	NV
		12Feb86	1767.5	159.1	26Mar87	2130.2	179.5			
		18May86	2216.7	184.6	29Sep87	2227.4	185.2			
1611+343	LPQ	12Feb86	2040.0	174.3	26Mar87	2831.7	222.0	30.1	10.6	V
		18May86	2277.9	188.2	29Sep87	3668.4	275.6			
		23Aug86	4210.0	311.2	11Jan88	4203.3	310.8			
1730−130	LPQ	11May85	6461.7	338.2	26Mar87	6035.0	317.9	12.0	4.6	V
NRAO 530		14Feb86	4656.7	253.4	29Sep87	5323.1	284.3			
		22Aug86	5916.8	312.3						
1741−038	LPQ	22Aug86	816.3	108.0	29Sep87	830.3	108.3	< 23.6	-1.3	NV
		27Mar87	903.8	109.7	10Jan88	760.2	107.0			
1748−253		27Mar87	815.6	115.2	29Sep87	727.8	112.2	< 33.8	-0.9	NV
2050+364	CD	03May85	2585.0	206.7	17Dec86	2438.3	197.8	< 12.2	-0.3	NV
		07Feb86	2224.5	185.1	27Mar87	2650.8	210.8			
		14May86	2195.8	183.4	09Jan88	2344.5	192.2			
		22Aug86	2551.7	204.7						
2128−123	LPQ	23Aug86	1447.5	123.4	28Sep87	1302.8	119.4	< 14.9	-0.3	NV
		17Dec86	1212.7	117.0	09Jan88	1466.1	124.0			
		27Mar87	1427.8	122.9						
2145+067		26Sep85	3277.8	192.0	27Mar87	2672.1	166.9	9.4	3.1	V
		23Aug86	3756.7	212.8	28Sep87	3272.1	191.8			
		18Dec86	3197.1	188.6	09Jan88	3340.0	194.7			
2155−152	BL	22Apr85	1744.7	132.7	23Aug86	2413.3	156.7	12.3	2.6	PV
		25Sep85	2008.2	141.7	28Sep87	2043.0	143.0			
		13May86	1582.2	127.5	09Jan88	2162.2	147.3			
2201+315	LPQ	26Apr85	1145.6	128.2	22Aug86	2420.0	196.7	28.0	7.2	V
		03May85	1252.1	133.0	26Mar87	1202.3	130.7			
		11Feb86	1818.2	161.9	28Sep87	1466.3	143.3			
		14May86	1028.3	123.2						
2223−052	HPQ	22Apr85	11501.9	583.7	17Dec86	11316.7	574.2	5.7	2.1	PV
3C446		27May85	13587.5	686.7	26Mar87	12585.7	637.2			
		25Sep85	11733.3	595.2	29Sep87	12988.3	657.1			
		14May86	11041.7	561.1	11Jan88	13240.0	669.5			
		22Aug86	12827.8	649.1						
2230+114	HPQ	26Apr85	6392.4	334.9	18Dec86	7809.2	403.1	12.6	6.8	V
CTA 102		03May85	8510.0	437.1	26Mar87	5482.0	291.8			
		07Feb86	6635.0	346.5	28Sep87	6618.0	345.7			
		14May86	7347.5	380.1	11Jan88	6011.1	316.8			
		22Aug86	7361.1	381.4						
2251+158	HPQ	25Apr85	12449.0	630.4	17Dec86	11194.4	568.6	10.6	3.4	V
3C454.3		03May85	12458.3	630.9	26Mar87	11544.4	585.8			
		29Sep85	11541.3	585.7	28Sep87	11799.9	598.4			
		11Feb86	11338.9	575.7	09Jan88	12473.0	631.6			
		14May86	8557.1	439.4						
2345−167	HPQ	27Apr85	2809.3	220.6	17Dec86	1850.6	163.7	12.4	3.2	V
		11Feb86	2534.5	203.7	26Mar87	2036.7	174.1			
		16May86	2217.9	184.7	28Sep87	2146.6	180.5			
		22Aug86	2774.6	218.5	09Jan88	2136.7	179.9			

Table 2. Flux-density measurements for the control and calibrator sample

Source	Type	Epoch	S_{327} (mJy)	Error (mJy)	Epoch	S_{327} (mJy)	Error (mJy)	m_c% (or $< v$%)	Γ
0023−263	Cal	28Apr85	16887.5	1186.4	25Sep85	18962.0	1331.1	< 16.1	0.3
0134+329	Cal	24Aug86	45462.5	3184.0	02Oct87	46843.8	3280.6	< 11.7	1.0
3C48		16Dec86	57775.0	4045.5	10Jan88	46075.0	3226.8		
		24Sep87	48125.0	3370.2					
0218−021	Cal	07Feb86	13154.2	665.3	18Dec86	12759.7	645.8	< 9.1	-1.0
3C63		24Aug86	12677.1	641.7	09Jan88	13626.7	688.6		
0300+107	Cont	03Apr87	840.4	108.5	09Jan88	777.8	107.3	< 28.9	0.7
		27Sep87	584.5	104.2					
0325+180	Cont	31Mar87	1514.0	145.7	09Jan88	1586.7	149.5	< 19.1	-1.4
		27Sep87	1459.8	143.0					
0350−073	Cal	12May85	10247.5	522.0	18Dec86	10471.0	533.0	< 7.3	-0.1
3C94		28Sep85	11446.8	581.0	27Mar87	10260.0	522.7		
		08Feb86	10875.3	552.9	28Sep87	10945.8	556.4		
		24Aug86	9742.7	497.3	10Jan88	10312.5	525.2		
0357+035	Cont	27Mar87	1043.9	112.8	10Jan88	826.7	108.2	< 23.1	0.1
		28Sep87	995.7	111.7	0.0				
0358+004	Cal	08Feb86	6258.0	328.5	27Mar87	6018.0	317.1	< 8.3	-2.0
3C99		24Aug86	5962.7	314.5	28Sep87	5925.0	312.7		
		18Dec86	6122.7	322.1	10Jan88	5898.1	311.4		
0359+055	Cont	27Mar87	2343.3	154.0	10Jan88	2007.8	141.7	< 14.0	2.3
		02Oct87	1783.3	134.0					
0406−180	Cal	26Mar87	5772.9	416.3	11Jan88	5685.0	410.3	< 14.3	-0.9
		28Sep87	5306.2	384.7					
0432+034	Cont	26Mar87	2062.7	143.7	28Sep87	2261.2	151.0	< 15.6	-0.1
0518+165	Cal	14May85	21900.0	1536.3	19Dec86	17859.4	1254.2	< 11.0	0.4
3C138		27Sep85	18550.0	1302.3	28Sep87	19494.3	1368.3		
		22Aug86	17450.0	1225.6	11Jan88	19300.0	1354.7		
0532+100	Cont	26Mar87	2688.9	167.6	11Jan88	3050.0	182.4	< 12.2	0.4
		28Sep87	2696.9	167.9					
0718+132	Cont	26Mar87	1239.4	117.7	10Jan88	1430.0	122.9	< 17.8	-0.5
		29Sep87	1361.3	121.0					
0732+332	Cal	09Feb86	6708.0	480.1	17Dec86	6567.5	470.5	< 11.3	-0.5
		16May86	6951.8	496.8	29Sep87	7249.6	517.2		
		22Aug86	6167.2	443.1	10Jan88	7168.8	511.7		
0741−063	Cal	15May85	10745.5	546.5	16May86	10418.8	530.5	< 8.0	-0.3
		26Sep85	9879.2	504.0	26Mar87	9379.2	479.5		
		09Feb86	10181.7	518.8	10Jan88	10195.0	519.5		
0758+143	Cal	26Sep85	9137.5	467.7	19Dec86	9698.4	495.1	< 17.7	-0.1
3C190		09Feb86	10040.2	511.9	05Oct87	10422.2	530.6		
		14May86	10280.7	523.7	10Jan88	9325.0	476.9		
		22Aug86	9515.4	486.2					
0840+184	Cont	26Mar87	1527.2	146.4	08Jan88	1590.4	149.7	< 18.6	-0.4
		29Sep87	1771.7	159.3					
0855+176	Cont	26Mar87	1499.5	145.0	03Oct87	1895.0	166.1	< 9.5	1.2
		26Sep87	1762.2	158.8					
0855+280	Cal	15May85	9180.0	650.3	29Sep87	8134.0	578.1	< 20.2	-0.3
3C210		30Sep85	8858.3	628.1	08Jan88	7160.0	511.1		
		26Mar87	7987.5	568.0					

Table 2. continued

Source	Type	Epoch	S_{327} (mJy)	Error (mJy)	Epoch	S_{327} (mJy)	Error (mJy)	m_c% (or < v %)	Γ
0909+165	Cont	26Mar87	4899.2	357.2	08Jan88	4598.3	337.1	< 14.5	-0.5
		05Oct87	5170.0	375.5					
0940+029	Cont	28Mar87	2988.3	179.8	08Jan88	2945.0	178.0	< 12.1	-1.4
		05Oct87	2840.0	173.7					
1140+223	Cal	25Apr85	12140.0	855.7	18Dec86	11671.4	823.1	< 11.1	-1.4
3C263.1		07Feb86	12429.2	875.8	20Mar87	11908.3	839.6		
		14May86	11385.7	803.3	08Jan88	11100.0	783.4		
1239−044	Cal	25Apr85	10868.3	552.5	22Aug86	10441.7	531.6	< 8.0	0.2
3C275		07Feb86	10687.5	543.7	20Mar87	11890.0	602.9		
		14May86	10566.1	537.7	08Jan88	11664.3	591.7		
1328+307	Cal	07Feb86	30292.9	2122.9	29Sep87	29901.8	2095.5	< 11.7	0.2
3C286		16May86	26999.4	1892.6	08Jan88	26433.3	1853.0		
		22Aug86	25675.0	1800.0					
1416+067	Cal	12Feb86	30061.1	1506.4	20Mar87	28268.8	1417.0	< 7.5	-1.2
3C298		16May86	27446.3	1376.0	29Sep87	30695.5	1538.0		
		22Aug86	29431.3	1475.0	10Jan88	28130.0	1410.1		
		25Dec86	29341.3	1470.5					
1436−167	Cal	28Apr85	5325.0	385.9	25Dec86	5670.3	409.3	8.7	2.4
		24Sep85	6455.0	462.8	24Mar87	5756.8	415.2		
		12Feb86	6137.0	441.1	29Sep87	5246.0	380.6		
		15May86	4474.4	328.8	10Jan88	6116.4	439.7		
		22Aug86	5743.2	414.3					
1517+204	Cal	12Feb86	9390.0	664.9	20Mar87	8013.5	569.8	< 11.1	-0.6
3C318		23Aug86	9295.0	658.3	29Sep87	8826.6	625.9		
		21Dec86	8759.8	621.3	10Jan88	9050.0	641.3		
1547+309	Cal	12Feb86	5130.0	372.8	26Mar87	5515.5	398.8	< 10.9	-1.7
		18May86	5305.4	384.6	29Sep87	5395.6	390.6		
		22Aug86	5390.0	390.3	10Jan88	5455.3	394.8		
		26Dec86	5829.4	420.1					
1643+022	Cal	14Feb86	6344.0	332.6	26Mar87	6681.7	348.7	< 9.5	-1.5
		23Aug86	6413.3	335.9	30Sep87	6356.8	333.2		
1756+134	Cal	14Feb86	6597.5	344.7	27Mar87	6741.3	351.6	7.8	2.7
3C365		18May86	7209.5	374.1	29Sep87	6271.3	329.1		
		22Aug86	6219.4	326.7	10Jan88	5491.7	292.2		
1828+487	Cal	14Feb86	37472.0	2625.0	17Dec86	41216.7	2886.9	15.2	4.8
3C380		18May86	41499.0	2906.7	26Mar87	34150.0	2392.6		
		22Aug86	41783.3	2926.5	10Jan88	28050.0	1966.0		
2244+366	Cal	11Feb86	5437.2	393.5	26Mar87	5078.9	369.3	< 11.4	-1.2
		13May86	5263.0	381.7	28Sep87	5524.2	399.4		
		23Aug86	5837.8	420.7	11Jan88	5478.9	396.4		
2252+129	Cal	07Feb86	9216.7	471.6	26Mar87	8155.0	419.8	< 8.1	0.2
3C455		13May86	7918.1	408.3	29Sep87	8672.3	445.0		
		23Aug86	8310.5	427.4	09Jan88	8162.5	420.2		
2314+038	Cal	29Apr85	17740.1	892.6	16May86	15585.0	785.6	< 7.3	1.9
3C459		03May85	19950.0	1002.5	23Aug86	18785.7	944.6		
		29Sep85	18381.3	924.5	27Sep87	18395.8	925.2		
		07Feb86	17822.2	896.7	09Jan88	17191.7	865.4		
2338+042	Cal	14Feb86	5703.5	302.2	28Sep87	5823.9	307.9	< 9.5	-2.2
		22Aug86	5777.5	305.7	09Jan88	5876.9	310.4		